소결공정에서의 완전소결점 위치제어

권 욱 현*, 고 명 삼*, 이 상 정*, 백 기 남**
* 서울대학교 공과대학 제어계측공학과 ** 포 항 제 철

Burnthrough Point Control for a Sintering Process

W.H. Kwon*, M.S. Ko*, S.J. Lee*, and K.N. Baek**
* Dept. of Control & Instrumentation Eng., Seoul National Univ., Seoul, Korea
** Pohang Steel Company, Pohang, Korea

Abstract

This paper treats the modelling and the control of the burnthrough point control system for an industrial sintering process. First, a state-space model is derived by defining new unconventional variables. A simple control law is proposed, which consists of the modified receding horizon control law and the least-squares prediction algorithm. The stability and the tracking properties of this control law are proved.

The real-time experiments are carried out in a POSCO sintering plant and satisfactory results are presented in this paper. Before the real-time experiments, computer simulations are done and their results are also given for the comparison with the real-time experiments.

I. INTRODUCTION

In recent years, many theoretical and simulation studies have been carried out concerning the application of modern control theories to industrial processes [1] - [5]. In this paper, the modelling and the control of the burnthrough point (BTP) control system of an industrial sintering process are investigated.

The sintering of iron ore in order to produce much improved blast-furnace materials is an essential part of modern iron-making processes, since the quality of sinter has a great effect on the operating condition of the blast-furnace. The control of sintering processes should lead to producing the sinter of the best possible quality while consuming as small energy as possible.

The sinter is prepared either by a batch process, e.g. in a Greenawalt machine, or by a continuous process using a Dwight-Lloyd type of machine which is adopted in most industrial sintering processes presently. A diagrammatic representation of an industrial sintering process with the Dwight-Lloyd sintering machine is shown in Fig.1. The raw matprial (usually referred to as 'raw mix') in the form of small pellets composed essentially of ore, coke, and water is loaded onto a moving grate and levelled to form a bed. Also included in the raw mix are return fines— pieces of sinter which are returned for reprocessing because they are too small. The grate is constructed from metal and refractory links, allowing a large fan to suck air down through the bed to the so-called wind boxes where the temperature of sucked air is measured, driving off the volatiles, and fusing the raw mix to form sinter. And then, the sinter is crushed and products of acceptable size are brought to the blast-furnace, while return fines are refeeded for reprocessing.

In control standpoints, the major control loops in Fig.1 consist of the feed control, the return fine/coke control, the water control, the burnthrough point (BTP) control, and the bed height control. Among these control loops, the burnthrough point control, which is treated in this paper, is the most important one since this control is related to the production rate and results in main sources of disturbances in other control loops. The purpose of this control is to keep the burnthrough point within an allowable range from a desirable set point. The existing mathematical models [6] - [8] are, however, too complicated for control purposes. Moreover, there exist few open literatures on the burnthrough point control methods.

This paper describes how the burnthrough point control system can be represented by a linear constant discrete-time state-space model. Based on this model, a simple controller is proposed, which consists of the modified receding horizon control law and the least-squares prediction algorithm. The prediction algorithm is used for predicting the burnthrough time in order to replace the permeability whose measurement is difficult and costs much. The control law was implemented on PDP 11/34 minicomputer in the POSCO (Pohang Steel Company, Korea) sintering plant IV, and improvements in the quality of sinter have been observed. Some of those experimental results are presented in this paper.

This paper is organized as follows. In Section II, the state-space model of the burnthrough point control system is derived. In Section III, the control law is presented and its properties are analyzed. In Section IV, the prediction algorithm is given. The real-time experiment and the simulation results are shown in Section V. Finally, some concluding remarks are given in Section VI.

II. Modelling of Burhthrough Point Control System

Based on the heat and mass flow, there exist some complex mathematical models [6] - [8] which

describe the solid and gas temperature, and the levels of materials such as the oxygen, the carbondioxide, the water, the limestone, and the coke. According to those models, the typical temperature history of a sinter package follows such a pattern as shown in Fig.2, the burnthrough time (BTT) is defined to be the time for a sinter package to reach the highest temperature. The burnthrough time and the temperature are all dependent on several process variables. Although those models in [6] - [8] are valuable in analyzing detail relationships among sintering process variables, they are inadequate for desigining the burnthrough point control laws for the dynamic (moving) sintering process (Fig. 3) because they describe the behavior of the static pilot plant (or the test pot) and are too complicated. Thus, a simpler dynamic model for the burnthrough point control systems is very important for real applications.

For precise understanding of the burnthrough point control problem, the burnthrough point of a given material moving on the strand is defined to be the point on the strand where the temperature of that material reaches its highest value. The burnthrough point control problem is to keep the burnthrough point of each material at the desirable fixed point. For the burnthrough point control problems, the input variable is the strand speed and the controlled variable is the burnthrough point of each moving material. The relationship between those two variables is very complicated. Let the material S be loaded on the bed at the time t_s and its burnthrough time BTT_s. Then the burnthrough point of that material has a distance, denoted by BTP_s, from the charging end of the strand :

$$BTP_s = \int_{t_s}^{t_s + BTT_s} v(t)dt, \qquad (2.1)$$

where t_s is a function of the history of the strand speed $v(\tau)$, $\tau \leq t_s$ and BTT_s depends on the material S. Thus, the burnthrough point control problem is to find $v(\cdot)$ such that BTP_s becomes a desirable constant value for all different S. The complicated conventional relationship like Eq. (2.1) is of little use for the solution, and thus we need another judicious approaches.

For the dynamic sintering process, we assume a large number of hypothetical windows which are fixed as in Fig.3. Let ℓ be the width of a window. The desired position of the burnthrough point is the position of the window n, that is, the distance of the disired burnthrough point from the charging end of the strand is $n\ell$. Here we use the nomenclature 'event' during which the strand moves a window distance ℓ. Let k be the number of events, u(k) the time duration of the kth event, and v(k) the average strand speed during the kth event. Then, we have

$$u(k) = \frac{\ell}{v(k)} \cdot \qquad (2.2)$$

The state $x_i(k)$ is defined as the time which the sinter package at the window i at the begining of the kth event has spent from the instant when it was loaded onto the strand. Since the sinter package at the window i at the beginning of the (k+1)th event lay at the window (i-1) at the beginning of the kth event and will spend u(k) during the kth event, we have the following relationships :

$$\begin{aligned} x_1(k+1) &= u(k), \\ x_2(k+1) &= x_1(k) + u(k), \\ &\vdots \\ x_i(k+1) &= x_{i-1}(k) + u(k), \\ &\vdots \\ x_n(k+1) &= x_{n-1}(k) + u(k). \end{aligned} \qquad (2.3)$$

Next, since the desired burnthrough point is the position of the window n, we take the controlled output y(k) as

$$y(k) = x_n(k). \qquad (2.4)$$

Thus, the state-space model for the burnthrough point control system is given by

$$x(k+1) = A\,x(k) + b\,u(k), \qquad (2.5.a)$$

$$y(k) = c\,x(k), \qquad (2.5.b)$$

where $x(k) \in R^n$ denotes the system state vector, $u(k) \in R^1$ the control input, and $y(k) \in R^1$ the output ; A, B, and C are given by

$$A = \begin{bmatrix} 000\ldots000 \\ 100\ldots000 \\ 010\ldots000 \\ \cdots\cdots\cdots \\ 000\ldots100 \\ 000\ldots010 \end{bmatrix}, \quad b = \begin{bmatrix} 1 \\ 1 \\ 1 \\ \vdots \\ 1 \end{bmatrix},$$

$$c = [00\ldots01] \qquad (2.6)$$

with appropriate dimensions.

Note that the state-space model (2.5) for the burnthrough point control system is of the dual phase-variable canonical form which is both completely controllable and completely observable. As shown in Fig.3, the temperature is measured in the windboxes. Therefore, we locate the hypothetical windows in such a way that they are aligned with the wind boxes, and measure the temperature at the beginning of each event. We have the following assumptions :

Assumption 1 : The temperature of sucked air in the windbox i at the beginning of the kth event represents the average temperature of the sinter package at the window i at the beginning of the kth event.

Assumption 2 : The average temperature of a sinter package follows the pattern shown in Fig. 2 while moving on the strand.

Since the suction speed of the fan is much faster than the strand speed, there exists no delay in the measurement. Therefore, Assumption 1 is reasonable. Assumption 2 is also true judging from the real measured data. The value y(k) is the time which the sinter package at the desired BTP at the beginning of the kth event has spent from the instant when it was loaded onto the strand. Let the burnthrough time of the sinter package at the window n at the beginning of the kth event denoted by $r_n(k)$. Then, the burnthrough point control problem can be interpreted as a problem to find u(k) such that it keeps y(k) as close to $r_n(k)$ as possible for all k. Note that since a sinter package moves the distance corresponding to the width of a window after each event, the burnthrough time of the sinter package at the window n at the beginning of the (k+M)th event will be that of the sinter package at the window (n-M) at the beginning of the kth event, that is,

$$r_n(k+M) = r_{n-M}(k) \quad . \qquad (2.7)$$

In reality, the reference vector r(k) consisting of burnthrough times of the sinter packages at the windows 1 ~ n is unknown. Hence, it must be predited from some measurements including the permeability. A simple control law is given in the next section in case r(k) is known. A prediction method for unknown r(k) is suggested in the following section.

III. A Simple Control Law

The burnthrough point control has two objectives :

1. If possible, make the output y(k) equal to the reference $r_n(k)$ for all k.
2. Keep the variation in the strand speed as small as possible.

The second objective is necessary since the variation in the strand speed is the main source of the disturbance in othe control loops. This control problem can be seen as a tracking problem, where the reference signal is $r_n(k)$. The standard tracking problem, however, requires to calculate the control signal minimizing $\sum_{i=0}^{\infty}$ [$e^T(i)Q\,e(i) + u^T(i)R\,u(i)$] and needs the solution of the Riccati equation, where e(i) = r(i)-y(i). The cost term Σ (u(i) - u(i-1))^T R(u(i)-u(i-1)) is more reasonable than the term $\Sigma\, u^T(i)$ R u(i) according to the objective 2. Moreover, the reference signal is unknown in practical situations. From these points, we consider another control law.

The state-constrained receding horizon control law with a standard cost $\Sigma\, u^T(i)R\,u(i)$ [9]-[11] has been known to be a simple but useful method for stabilization problems. In this paper, we suggest a output-constrained receding horizon control law with a non-standard cost Σ (u(i)-u(i-1))^{T}R(u(i)-u(i-1)). In spite of the output constraint and the nonstandard cost, good properties such as stability, tracking, and simplicity will be obtained.

We will find a control law for the system (2.5) which minimizes a cost functional

$$J(u) = \sum_{i=1}^{k+M-1} (u(i)-U(i-1))^T R(u(i)-u(i-1)) \qquad \text{------(3.1)}$$

with the constraint

$$y(k+M) = r_n(k+M). \qquad (3.2)$$

Since the cost functional (3.1) is not standand, we introduce the new state $\bar{x}(k)$ and the new control $\bar{u}(k)$ defined by

$$\bar{x}(k) = \begin{bmatrix} x(k) - x(k-1) \\ y(k) \end{bmatrix}, \qquad (3.3)$$

$$\bar{u}(k) = u(k) - u(k-1) \; . \qquad (3.4)$$

The augmented system is represented by

$$\bar{x}(k+1) = \bar{\bar{A}}\bar{x}(k) + \bar{\bar{b}}\bar{u}(k), \qquad (3.5.a)$$

$$y(k) = \bar{c}\bar{x}(k), \qquad (3.5.b)$$

where

$$\bar{\bar{A}} = \begin{bmatrix} A & 0 \\ CA & 1 \end{bmatrix}, \quad \bar{\bar{b}} = \begin{bmatrix} b \\ 1 \end{bmatrix}, \text{ and } \bar{c} = [0 \; c]. \qquad (3.6)$$

For this system, we will find a control law which minimizes the cost functional

$$J(\bar{u}) = \sum_{i=k}^{k+M-1} \bar{u}^T(i)R\,\bar{u}(i) \qquad (3.7)$$

with the constraint (3.2), where R > 0 and M > 0. A little modification of [10] can give the solution to this problem :

$$\bar{u}(k) = -R^{-1}(\bar{c}\,\bar{\bar{A}}^{M-1}\,\bar{\bar{b}})^T W^{-1}(M) \cdot [\bar{c}\,\bar{\bar{A}}^M\,\bar{x}(k) - r_n(k+M)], \qquad (3.8)$$

where

$$W(M) = \sum_{i=0}^{M-1} \bar{c}\,\bar{\bar{A}}^{M-i-1}\,\bar{\bar{b}}\,R^{-1}(\bar{c}\,\bar{\bar{A}}^{M-i-1}\,\bar{\bar{b}})^T \qquad (3.9)$$

Using the matrices in the equation (3.6), we can see that

$$\bar{c}\,\bar{\bar{A}}^i\,\bar{\bar{b}} = \begin{cases} i+1, & 0 \le i \le n-1 \\ n, & i \ge n \end{cases}, \qquad (3.10)$$

$$W(M) = \frac{1}{R}\,\frac{M(M+1)(2M+1)}{6}, \qquad (3.11)$$

$$\bar{c}\,\bar{\bar{A}}^M = [0 \ldots 0 \underbrace{1 \ldots 1}_{\leftarrow M \rightarrow} 0\; 1], \qquad (3.12)$$

and

$$\begin{aligned} \bar{c}\,\bar{\bar{A}}^M\,\bar{x}(k) &= (x_{n-M}(k) - x_{n-M}(k-1)) \\ &\quad + (x_{n-M+1}(k) - x_{n-M+1}(k-1)) \\ &\quad + \ldots + (x_{n-1}(k) - x_{n-1}(k-1)) \\ &\quad + y(k) \\ &= x_{n-M}(k) + M\,u(k-1) \; . \end{aligned} \qquad (3.13)$$

Note that the horizon distance M is a design parameter. The larger M will result in less variation in control but slower response speed in the burnthrough point, while the smaller M will result in more variation in control but faster response speed in the burnthrough point. Since the state at n events after the present kth event can not be calculated, the horizon distance M must be less than n for this problem. With 0 < M < n, the control law (3.8) is simplified using the relations (3.10) - (3.13) :

$$u(k) - u(k-1) = \frac{-6}{(M+1)(2M+1)}[\, x_{n-M}(k) - r_n(k+M) + M\,u(k-1) \,]. \qquad (3.14)$$

Thus we have

$$u(k) = (1 - M\alpha)\,u(k-1) + \alpha(r_{n-M}(k) - x_{n-M}(k)), \qquad \text{------- (3.15)}$$

where

$$\alpha = \frac{6}{(M+1)(2M+1)} \quad . \qquad (3.16)$$

This receding horizon control law is simple and easy to install in the digital computer. It is known that the closed-loop system in asymptotically stable under the state-constrained receding horizon control law if M > n and the state feedback is applied [9]. In this paper, however, we have taken the horizon distance M less than n by practical considerations. Also, the output constraint (3.2) is introduced in stead of the state constraint. Thus, the closed-loop stability remains to be proved. The block diagram of the control system is shown in Fig.5, where d represents the disturbance due to the motor load change, the calculation error, and the temperature measurement noise. In Fig.5, we use the relationship

$$x_{n-M}(k) = c\,A^{M}\,x(k), \qquad (3.17)$$

where $c\,A^{M} = [\,0 \ldots 0\ 1\ 0 \ldots 0\,]$ with unity (n-M)th element. The system (2.5) and the control (3.15) can be represented in the z-domain by

$$z\,X(z) = A\,X(z) + b\,U(z), \qquad (3.18)$$

$$U(z) = \frac{\alpha}{1-(1-M\alpha)z^{-1}}\,c\,A^{M}(R(z) - X(z)), \qquad (3.19)$$

where X(z), U(z), and R(z) are the z-transforms of x(k), u(k), and r(k), respectively. The closed-loop stability is determined by the characteristic polynomial :

$$p(z) = \det\left(zI - A + \frac{\alpha}{1-(1-M\alpha)z^{-1}}\,b\,c\,A^{M}\right). \qquad (3.20)$$

After some algebraic treatments, the equation (3.17) becomes

$$p(z) = \frac{z^{M+1}[z^{n-M} + (M\alpha+\alpha-1)z^{n-M-1} + \alpha z^{n-M-2} + \ldots + \alpha z + \alpha]}{z - (1-M\alpha)} \quad . \qquad (3.21)$$

The denominator and the numerator polynomials of the equation (3.21) have no common factor except in the case of M = n. Therefore, the closed-loop stability depends on whether all the roots of the following equation lie within the unit disc or not :

$$z^{n-M} + (M\alpha+\alpha-1)z^{n-M-1} + \alpha z^{n-M-2} + \ldots + \alpha z + \alpha = 0. \qquad (3.22)$$

Theorem 3.1 : The control law (3.15) stabilizes the system (2.5) for $2 \leq M < n$. Moreover, if the reference signal r(k) is a step signal, then the steady-state error is zero.

Proof : From Jury's stability test, it can be shown that all the roots of the equation (3.22) lie within the unit disc in the z-plane for $2 \leq M < n$. The error e(k) is defined by

$$e(k) = r_n(k) - y(k) \quad . \qquad (3.23)$$

Let the disturbance d(k) ≡ 0 in Fig.5. Then the relation between the error and the reference is

$$E(z) = c\,(R(z) - X(z))$$

$$= c\,\left[\, I - \frac{\alpha}{1-(1-M\alpha)z^{-1}} \cdot \left(zI - A + \frac{\alpha}{1-(1-M\alpha)z^{-1}}\,b\,c\,A^{M} \right)^{-1} b\,c\,A^{M} \,\right] R(z) \quad . \qquad (3.24)$$

After some algebraic calulation, it can be shown that

$$E(z) = \left[\, 1 - \frac{\frac{\alpha}{1-(1-M\alpha)z^{-1}}\,\frac{1-z^{n}}{1-z}}{z^{n} + \frac{\alpha}{1-(1+M\alpha)z^{-1}}(z^{M} + z^{M+1} + \ldots z^{n-1})} \,\right] R(z) \qquad \text{----- (3.25)}$$

Therefore, the steady-state error becomes

$$e(\infty) = \lim_{z\to 1}\left[\, 1 - \frac{\alpha(1+z+\ldots+z^{n-1})}{z^{n}+(M\alpha+\alpha-1)z^{n-1}+\alpha(z^{n-2}+\ldots+z^{M})} \,\right] R_0$$

$$= 0 \qquad (3.26)$$

for the step reference signal

$$R(z) = \frac{R_0}{1-z^{-1}} \quad . \qquad (3.27)$$

This completes the proof.

It is noted that for the system (2.5), the control law which minimizes $\sum_{i=k}^{k+M-1} u(i)R\,u(i)$ with the constraint (3.2) can be shown to be given by

$$u(k) = \frac{1}{M}\left(r_{n-M}(k) - x_{n-M}(k) \right) \qquad (3.28)$$

for $0 < M < n$. The closed-loop system under this control law can be also shown to be asymptotically stable. And, the steady-state error for a step reference signal (3.27) is

$$e(\infty) = \lim_{z\to 1} c\,\left(I - \frac{1}{M}(zI - A + \frac{1}{M}bcA^{M})^{-1}\,bcA^{M}\right)R_0$$

$$= \lim_{z\to 1}\left(1 - \frac{1+z+\ldots+z^{n-1}}{Mz^{n}+z^{n-1}+\ldots+z^{M}}\right)R_0 = 0,$$

which is the same result as for the control law (3.15). But the control law (3.28) is inferior to the control law (3.15) in practical viewpoint, namely, the requirement of small variations in control.

IV. Prediction of Reference Signal

In our model, the burnthrough time of the sinter package is the reference or the command signal. Therefore, the burnthrough time must be decided before the control law is activated.

That is to say, $r_{n-M}(k)$ in the equation (3.15) which is the burnthrough time of the material at the window (n-M) at the beginning of the kth event, must be estimated.

The burnthrough time depends mainly on the ingredients of materials, the permeability, the amount of water, the bed height, and the suction speed, where the bed height and the suction speed are usually constant during the operation. In practice, the permeability is known to be the most important factor, and thus the burnthrough time is predicted by measuring the permeability of the raw mix at the first window. The permeability, however, is very difficult to measure. And since the ingredients of raw mix or the permeability changes slowly, we predict the burnthrough time from the history of the measured burnthrough times. We adopt the least-squares algorithm with covariance resetting [12] for predicting $r_{n-M}(k)$. The prediction model for the least-squares algorithm must be determined from both the degree of fitting and the complexity of computation. The higher order of the model will result in better fitting but larger computation time which is unacceptable for real-time applications. We predict $r_{n-M}(k)$ from measurable $r_n(k)$ and $r_{n+M}(k) = r_n(k-M)$ shown in Fig.6. In order to compute the burnthrough time $r_\ell(k)$ for $\ell > n$, the temperature history of the sinter package is measured, from which the burnthrough time is computed from the definition. Let $z(k)=r_{n-M}(k)$, $z(k-1) = r_n(k)$, and $z(k-2) = r_n(k-M)$. We assume the burnthrough time follows the stochastic autoregressive model :

$$\begin{aligned} z(k) - \bar{r} &= \alpha(k)\,(z(k-1)-\bar{r}) + \beta(k)\,(z(k-2)-\bar{r}) \\ &\quad + w(k) \\ &= \phi^T(k-1)\,\theta(k), \end{aligned} \qquad (4.1)$$

where

$$\phi(k-1)^T = [\, z(k-1)-\bar{r},\ z(k-2)-\bar{r}\,], \qquad (4.2)$$

$$\theta(k)^T = [\, \alpha(k),\ \beta(k)\,], \qquad (4.3)$$

and w(k) is a white noise sequence, z(k-1) and z(k-2) are known burnthrough times of processed sinter packages, and $\bar{r}$ is the mean value of the known burnthrough times. Here, $\hat{\theta}(k)$ is calculated by the least-squares algorithm with corariance resetting [12] :

$$\hat{\theta}(k) = \hat{\theta}(k-1) + \frac{P(k-2)\phi(k-1)}{1 + \phi(k-1)^T P(k-2)\phi(k-1)} \cdot [\, z(k) - \bar{r} - \phi(k-1)^T \hat{\theta}(k-1)] \qquad (4.4)$$

with $\hat{\theta}(0)$, $p(-1) > 0$ given. Let $\{K_s\} = \{k_1, k_2, \ldots\}$ be the times at which resetting occurs ; then for $k \notin \{K_s\}$ an ordinary sequential least-squares update is used : that is,

$$P(k-1) = P(k-2) - \frac{P(k-2)\phi(k-1)\phi(k-1)^T P(k-2)}{1 + \phi(k-1)^T P(k-2)\phi(k-1)}. \qquad (4.5)$$

Otherwise, for $k = k_i \in \{K_s\}$, $P(k_i-1)$ is reset. Then, the predicted burnthrough time is given by

$$\hat{r}_{n-M}(k) = \hat{z}(k) = \phi(k-1)^T \hat{\theta}(k) + \bar{r}\ . \qquad (4.6)$$

The predicted signal (4.6) will be used for the calculation of the control law (3.15) :

$$u(k) = (1-M\alpha)u(k-1) + \alpha[\hat{r}_{n-M}(k) - x_{n-M}(k)]. \qquad (4.7)$$

In the next section, some prediction results will be shown using the real plant data of POSCO sintering plant IV. It will be observed that the prediction errors are very small even in case when the burnthrough time varies rampwise, which exhibits the good property of tracking time-varying parameters as expected.

V. Experiments

The simple control law (3.15) with the predicted reference signal (4.6) has been applied to the PSOCO (Pohang Steel Company) sintering plant IV, where the Dwight-Lloyd sintering machine is adopted (Fig.1). The length of the sinter strand is 100m. There exist 25 windboxes each of which has 4m width. We assume hypothetical 50 windows so that two windows are aligned with each windbox and ℓ = 2m. The desired position of the burnthrough point is 93.4m from the ignition point. We take the horizon distance M = 11. The parameters used in experiments are listed on Table 1. The flow of the control algorithm is as follows :

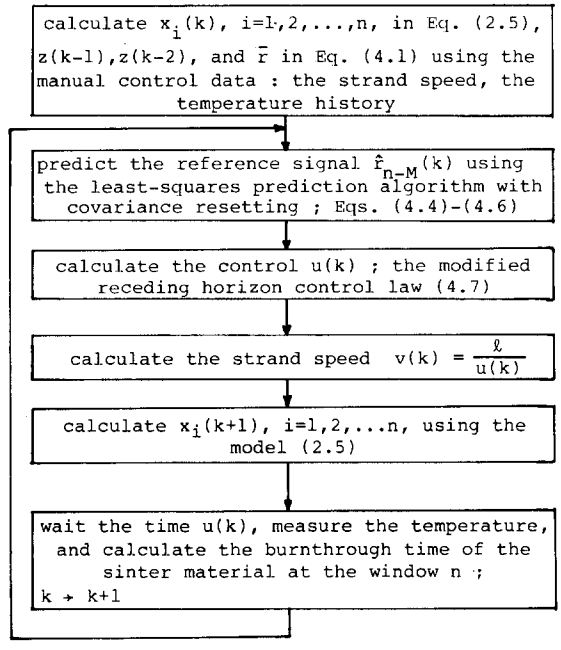

Before applying the control law (4.7), the prediction of reference signal has been tested using the recorded real plant data of POSCO sintering plant IV as shown in Fig.7. The prediction errors are within 10 seconds even in case when the burnthrough time varies rampwise, which exhibits the good tracking property of the prediction algorithm. For practical systems, the strand speed is proportional to the motor speed

which is controlled by the voltage input. Since the strand moves slowly, approximately at the speed of 100m/30min, and the motor has good tracking property by feedback loop, we consider the input voltage is proportional to the motor speed and thus to strand speed. Once u(k) is determined from the equation (4.7), the average strand speed during the kth event is obtained by $v(k) = \frac{\ell}{u(k)}$ from the equation (2.1). This value is applied to the motor drive system.

The experimental results are shown in Fig.9, and the parameters used in the experiments are list on Table 1. It is observed that the error between the measured burnthrough point and the desired burnthrough point is such that

mean = 71.78 cm,

standard deviation = 10.0 cm.

Note that the steady-state error should be zero following the properties of the proposed controller discussed in Section III. However, there exist some disturbances in our control system, and this leads to the above steady-state error amounting to 70 cm approximately. This can be analyzed as follows. Since the control algorithm is calculated by integer operation, there exist some round-off errors. The prediction of the reference signal has deviations from real value. Besides these, the motor load change and the temperature measurement error act as disturbances. Therefore, the steady-stat error in the burnthrough point can be written as

$$e_{BTP}(\infty) = -\tilde{v}(\infty)\, M\, d_0 , \qquad (5.1)$$

where d_0 denotes the disturbances, $\tilde{v}(\infty)$ is the steady-state strand speed. Using the experimental data, it is given that

$$d_0 = \frac{\ell}{\hat{v}(\infty)} - \frac{\bar{r}}{n} = -1.45, \qquad (5.2)$$

where $\bar{r}$ in the mean value of the real burnthrough time. Therefore, the steady-state error in the burnthrough time is calculated as follows

$$e_{BTP}(\infty) = \frac{318}{60} \times 11.7 \times 1.45 \cong 90 \text{ cm}, \qquad (5.3)$$

which approximates to the experimental result 71.78 cm

In Fig.10, the manual control results performed by expert operators are shown. From the table 2 concerning the statistics of the manual control results and the computer control results, improvements in the standard deviation both of the burnthrough point error and of the strand speed can be observed. Thus, it can be concluded that the controller proposed in this paper exhibits a better control performance than the manual control. Shown in Fig.11(a) is the simulation result using the real plant data. Since the floating-point operation is used in simulation, it is observed that the steady-state error becomes near zero as expected. In Fig.11(b), the simulation result using the integer operation is shown. Fig.11(b) shows about 77 cm steady-state error which is nearly identical with the experimental result in Fig.9.

In spite of the steady-state error amounting to 70 cm due to the disturbances discussed above, the burnthrough point occurs at the window where the desired burnthrough point locates. Therefore, it is concluded that the proposed controller shows a satisfactory performance.

VI. Conclusion

This paper treats the modelling and the control of the burnthrough point control system. Specifically, a simple model and a simple control law are suggested, which are not only stable but has good tracking property for real applications. The approach introduced in this paper is systematic and theoretic compared with the existing heuristic burnthrough point control methods.

It is shown that, by defining new variables, the burnthrough point control system can be modelled to the phase-variable canonical form which is both completely controllable and observable. In the model, the reference signal is the burnthrough time and the controlled output is the time for a sinter package to have spent on reaching the window at the desired burnthrough point. The state variables are the times for sinter packages to have spent on reaching their positions from the instant when loaded onto the strand, and the input is the time for sinter packages to spend on moving a window distance .

For the known reference signal, a simple but stable control law (3.15) is based on the modified receding horizon control with the output constraint (3.2) and minimum control variations (3.7). The stability and the tracking properties are proved.

For the unknown reference signal, a prediction method of the reference signal is suggested, which is based on the least-squares algorithm with covariance resetting. This alleviates the necessity of the very difficult permeability measurement, which cuts down the expenses. This prediction method combined with the modified receding horizon control law (3.15) results in the control law (4.7).

The control law introduced in this paper was applied to the real POSCO sintering plant IV which produces 3,840,000 tons of sinter a year. The performance was satisfactory and much better than that of manual control done by expert operators.

References

[1] T. Westerland,"A digital quality control system for an industry dry process rotary cement kiln," IEEE Trans. Automat. Contr., vol.AC-25, pp.885-890, Aug., 1981

[2] C. Greco, G. Menga, E. Mosca, and G. Zappa, "Performance improvements of self-tuning controllers by multistep horizons:The MUSMAR approach," Automatica, vol.20,pp.681-700, Sept., 1984

[3] K. J. Astrom,"Theory and applications of adaptive control — A survey," Automatica, vol.19, pp.471-486, Sept., 1983

[4] E. J. Davison,"Control of commercial heat exchanger using tuning regulators," IEEE Trans. Automat. Contr., vol.AC-25, pp.361-375, Jun., 1980

[5] Y. Thomas et al.,"Analysis of a DDC experiment based on state space methods," J. of Dynamic Systems, Measurement, and Control, Trans. ASME, vol.98, pp.324-331, Sept., 1976

[6] R. W. Young,"Dynamic model of sintering process," Ironmaking & Steelmaking, pp.25-31, 1978
[7] I. R. Dash and E. Rose,"Simulation of a sinter strand process," Ironmaking & Steelmaking, pp.321-328, 1977
[8] R. W. Lewis et al., Numerical Methods in Heat Transfer, vol. II, pp.485-510, John Wiley & Sons, New York, 1983
[9] Y. Thomas,"Linear quadratic optimal estimation and control with receding horizon," Electronic Letters, vol.11, pp.19-21, Jan., 1975
[10] W. H. Kwon and A. E. Pearson,"A modified quadratic cost problem ans feedback stabilization of a linear system," IEEE Trans. Automat. Contr., vol.AC-22, pp.838-842, Oct., 1977
[11] W. H. Kwon, A. M. Bruckstein, and T. Kailath, "Stabilizing state-feedback design via the moving horizon method," Int. J. Contr., vol. 137, pp.631-643, 1983
[12] G. C. Goodwin and K. S. Sin, Adaptive Filtering, Prediction, and Control, Prentice Hall, New York, 1984

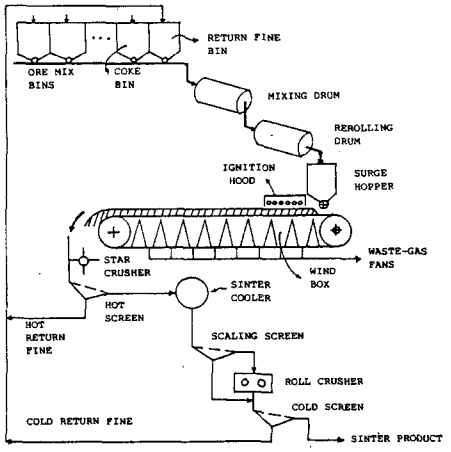

Fig.1 The Systematic Diagram of POSCO Sintering Plant IV

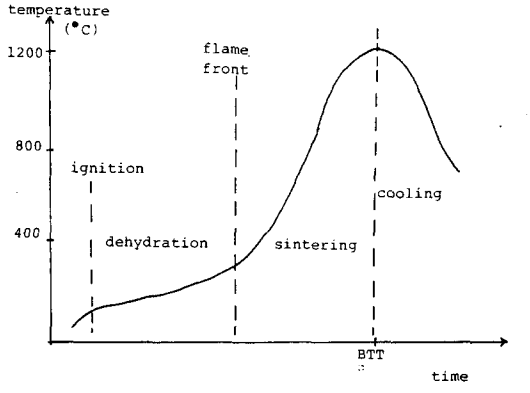

Fig.2 A Typical Temperature Pattern of Sintering Processes

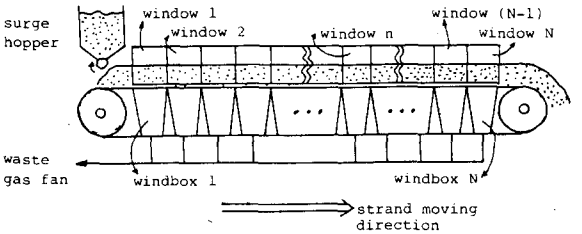

Fig.3 Hypothetical Window Structure and Sinter Bed Represented by a series of test pots

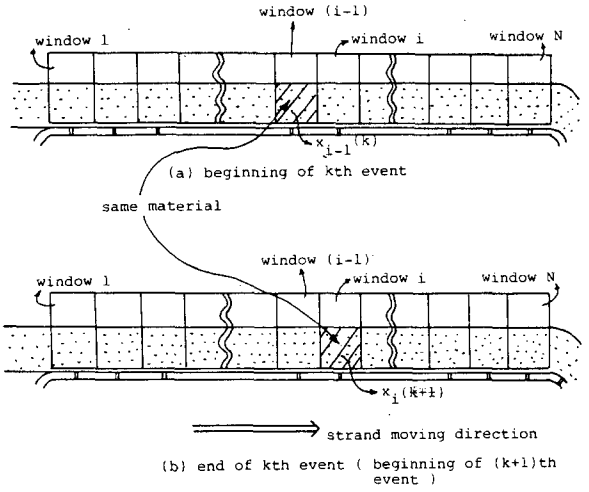

Fig.4 The Flow of Sinter Packages and the Definition of the State Variable

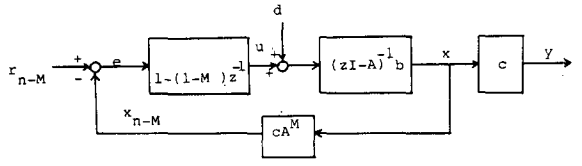

Fig.5 The Block Diagram of the Control System

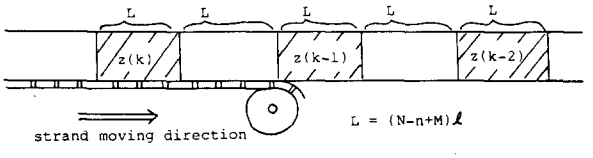

Fig.6 Assumption on Burnthrough Time

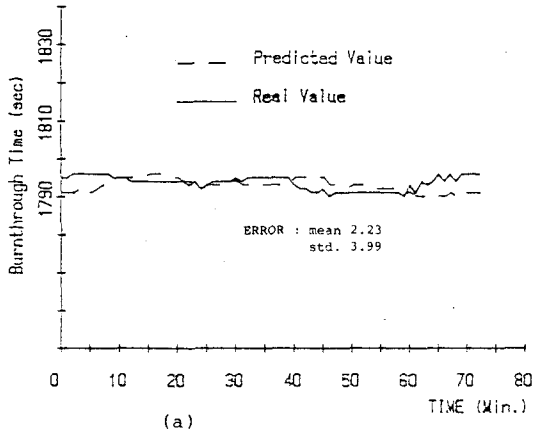

(a)

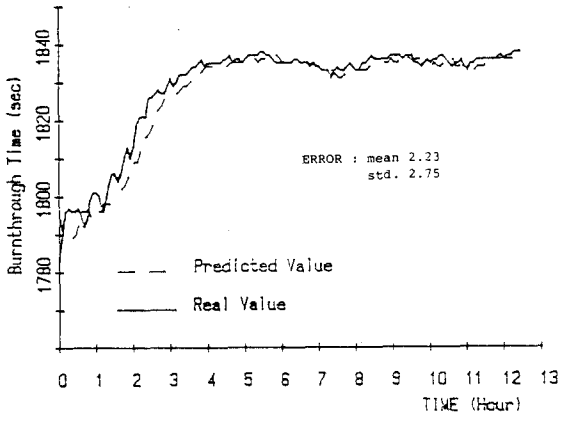

(b)

Fig.7 Prediction Results for Burnthrough Times

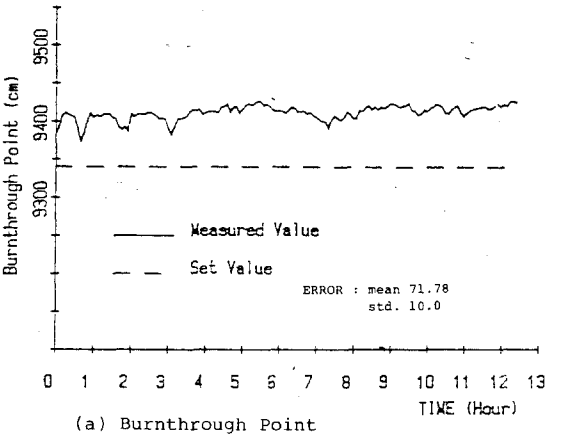

(a) Burnthrough Point

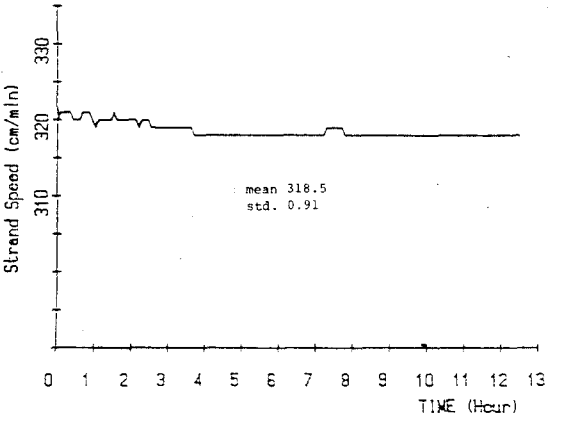

(b) Strand Speed

Fig.9 Experimental Results of the Proposed Control Law

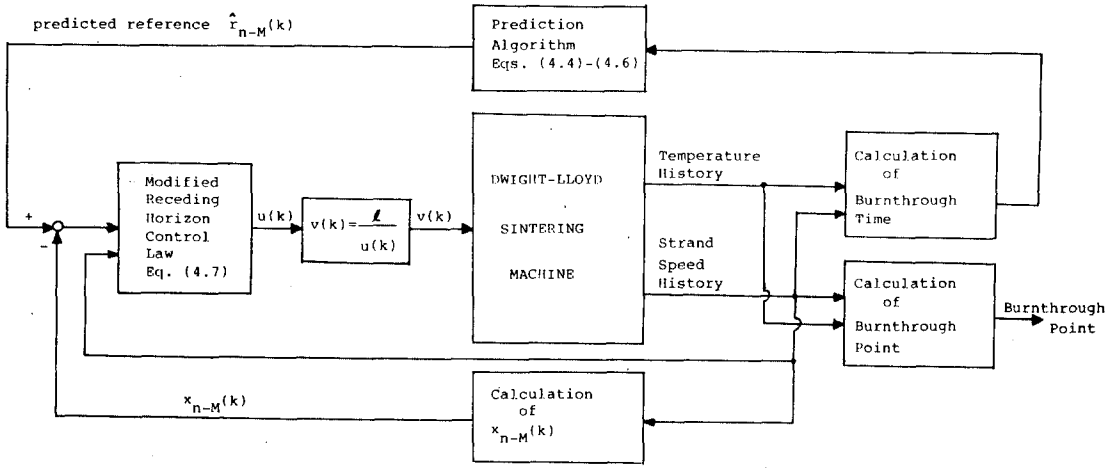

Fig.8 Real Implementation of the Proposed Control Law

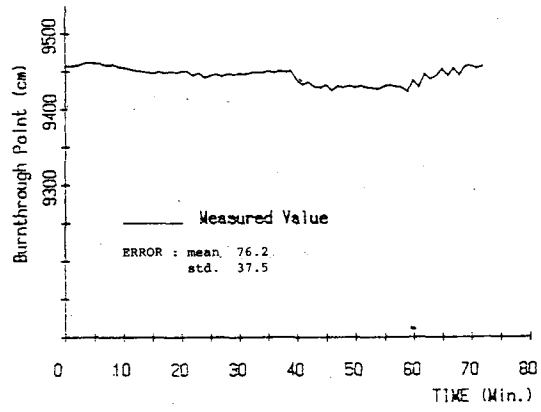

(a) Burnthrough Point

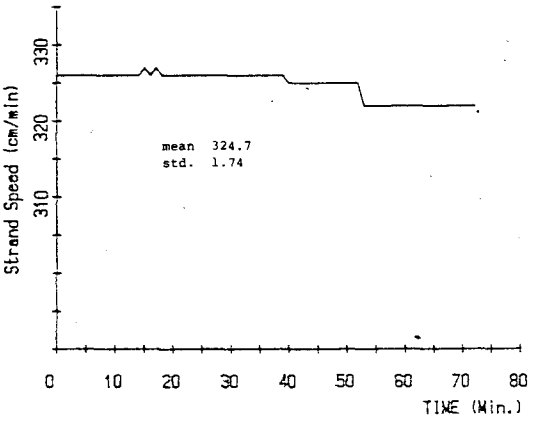

(b) Strand Speed

Fig.10 Manual Control Results

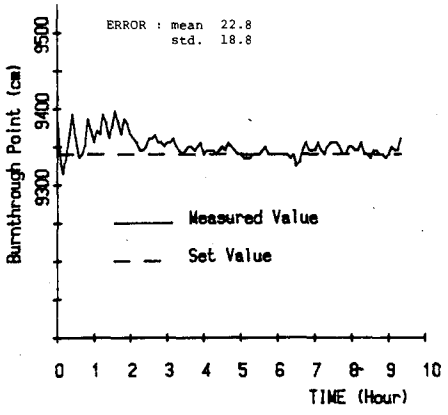

(a) Floating Point Operation

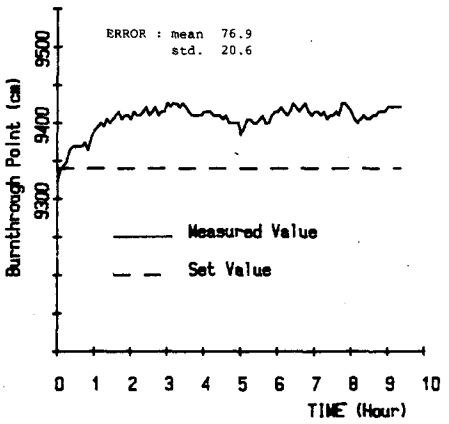

(b) Integer Operation

Fig.11 Simulation Results of the Proposed Control Law

Table 1 : Parameter Values used in Experiment

Parameter	Value	Reference
$\hat{\alpha}(0)$	0.6	Eq. (4.4)
$\hat{\beta}(0)$	0.3	Eq. (4.4)
Initial Value of Covariance	$\begin{bmatrix} 0.003 & 0.001 \\ 0.001 & 0.002 \end{bmatrix}$	Eq. (4.4)
Covariance Resetting Period	20 Steps	Eq. (4.5)
Number of Windows	50	Fig.3
Set Value of Burnthrough Point	93.4 m	
Horizon M	11	Eq. (4.7)

Table 2 : Statistics of Experimetal Results

	Manual Control		Proposed Control Law	
	Error in Burnthrough Point	Strand Speed	Error in Burnthrough Point	Strand Speed
mean	76.19	324.7	71.78	318.6
standard deviation	37.5	1.74	10.0	0.91